Supplemental information

CREBH normalizes dyslipidemia and halts atherosclerosis in diabetes by decreasing circulating remnant lipoproteins

Masami Shimizu-Albergine[1], Debapriya Basu[3], Jenny E. Kanter[1], Farah Kramer[1], Vishal Kothari[1], Shelley Barnhart[1], Carissa Thornock[1], Adam E. Mullick[4], Noemie Clouet-Foraison[1], Tomas Vaisar[1], Jay W. Heinecke[1], Robert A. Hegele[5,6,7], Ira J. Goldberg[3], Karin E. Bornfeldt[1,2]

Supplemental Methods

Mouse model of pre-diabetes. Male LDL receptor-deficient (*Ldlr*$^{-/-}$) *Gp*^{Tg} mice were injected with either empty control AAVDJ/8 (cAAV) or CREBH AAV (0.25×10^{11} and 1×10^{11} GC) containing a liver-selective promoter (TBG). One week prior to AAV injection, the mice were fed a low fat semi-purified diet. After AAV injection, the mice were kept on this diet for 4 weeks, and were then switched to a diabetogenic diet with added cholesterol (DDC; Subramanian et al., 2008) and maintained for 16 weeks. Body weight was monitored through the protocol. Blood was collected from the saphenous vein every 3-6 weeks for measurements of plasma TG, cholesterol and glucose. For glucose and insulin tolerance tests, mice were fasted for 4 h and then injected i.p. with 1 g glucose/kg BW or 0.75 U insulin/kg BW, respectively, and blood was collected at 0, 15, 30, 60 and 120 min. At the end of the study, blood was collected and plasma was immediately isolated. Livers and intestines were collected, snap-frozen and stored at -80°C prior to analysis. Heart and aorta were collected and fixed in formalin.

Analysis of peritoneal macrophages. Resident macrophages from the peritoneal cavity were collected and allowed to adhere for 1 h. Non-attached cells were washed off. The attached cells were then harvested for measurements of cholesteryl esters (Amplex Red Cholesterol assay, ThermoFisher, Grand Island, NY).

Flow cytometry of blood monocytes and neutrophils. Mice were bled from the retro-orbital plexus under isoflurane sedation after 4 weeks of diabetes. EDTA was used as an anti-coagulant. Total leukocytes were measured using an automated cell counter for mouse blood samples (Hemavet; Drew Scientific, Oxford, CT). For flow cytometric analysis, erythrocytes were lysed with an ammonium-chloride-potassium buffer and discarded, and leukocytes were stained using a fixable viability dye, CD45, CD115, and GR1 (eBioscience, now ThermoFisher). Monocytes were identified as CD115-positive cells, and neutrophils were identified as CD115-negative GR1^{hi} cells. All analyses were performed with live, single, CD45-positive cells. The monocytes were further divided into GR1^{hi} (Ly6C^{hi}) and GR1^{lo} (Ly6C^{lo}) subpopulations. The cells were analyzed on a BD

FACS RUO flow cytometer (BD Bioscience, Franklin Lakes, NJ). Flow cytometric data were normalized to total white blood cell counts (WBC) and expressed as cells/ml of blood, using the assumption that all WBC are CD45-positive.

Isolation of lipoprotein particles. TRL particles devoid of chylomicrons (density <1.019 g/mL), which contains VLDL and IDL as well as chylomicron remnants, were isolated from EDTA anti-coagulated plasma for the differential ion mobility analysis and LC-MS/MS analysis. First, chylomicrons were floated from 100 µl of plasma by a slow speed (3220g) spin for 30 min and the infranatant was collected. Density of the infranatant was adjusted with 1.063 g/ml KBr and saline to 1.019 g/ml and spun at 385,840g for 16.5 h. The top 75 µl was collected and dialyzed against 20 mM ammonium acetate, pH 7.0, in a 96-well flow dialyzer overnight.

HDL was isolated from 50 µl of plasma after adjusting the density with KBr to 1.21 g/mL and a 5.5 h spin at 385,840g. The top 100 µl was collected and 30 µl was dialyzed against 20 mM ammonium acetate, pH 7.0, for differential mobility analysis. The remaining 67 µl was further adjusted with saline to a density of 1.063 g/ml and spun at 385,840g for 2.5 h to sink HDL. The isolated particles were analyzed by differential mobility analysis within 2 days or aliquoted and immediately frozen for the LC-MS/MS analysis.

Analysis of HDL and TRL particle concentration. HDL and the VLDL+IDL particle concentration was quantified by calibrated ion mobility analysis on a differential mobility analyzer (DMA) (TSI Inc., Shoreview, MN). In mice, HDL exists primarily as one particle population. Total HDL was fitted to the DMA profiles by unsupervised, iterative curve-fitting (Hutchins et al., 2014). The particle concentration was calculated from the fitted peak areas using glucose oxidase as a calibrator. For total HDL particle concentration, intra-day and inter-day coefficients of variation were <10%. For the TRL analysis (<1.019 g/mL) the DMA analysis quantifies IDL particles as particles with diameters 24-28 nm and VLDL particles as broad peak with diameters 35-70 nm. An unsupervised peak-fitting algorithm was optimized with >50 individual samples. The particle concentration was calibrated using carefully characterized LDL particles. The inter-day and intra-day precision of the assay is <15% CV for combined IDL+VLDL particles.

Analysis of HDL cholesterol efflux capacity. HDL was isolated by sequential ultracentrifugation, as described above. J774 murine macrophages were incubated in Dulbecco's modified Eagle medium supplemented with 0.1% (wt/vol) fatty acid-free albumin (Dulbecco's modified Eagle medium + fatty acid-free albumin), [^{3}H]-cholesterol (0.5 µCi/ml), and an ACAT inhibitor (34.4 µmol/l; Sandoz) in 48-well tissue culture plates for 24 h at 37°C in a 5% CO_2 atmosphere. The cells were washed once with PBS and incubated in Dulbecco's modified Eagle medium + fatty acid-free albumin with and without 8CPTcAMP (0.3 mM; Sigma) for 24 h. Cells were washed again with PBS and then incubated with HDL for 4 h. The assays were performed using the same number of HDL particles/sample (corresponding to ~4 µg protein). The media were collected, any cell debris and dead cells were removed by filtration on 0.2 µm filter plates and the radioactivity was determined using a scintillation counter. The total cell counts were determined after lysing the cells in 0.1 N NaOH. Cholesterol efflux capacity was

calculated as ^{3}H-counts in the cultured media corrected for the counts in media without HDL and normalized to total cell counts.

Mouse plasma digestion for targeted mass spectrometry. Digestion of plasma samples was performed as previously described (Chait et al., 2020). Briefly, 3 µl of plasma was diluted 20x in 100 mM NH_4HCO_3 and further adjusted to 0.5% sodium deoxycholate (SDC) in 100 mM NH_4HCO_3, spiked with 0.05 µg of ^{15}N-APOA1 and a mixture of stable isotope labeled (SIL) peptides for the following proteins – APOA1, APOA4, APOB100, APOC1, APOC2, APOC3, and APOE. The samples were reduced with dithiothreitol (DTT) (30 min at 60°C) and alkylated with iodoacetamide (IAA) (45 min at room temperature in the dark). To remove unreacted IAA, more DTT was added and the samples were digested with 3 µg of trypsin (Worthington Biochemical Corp, Lakewood, NJ) (~ 1:10 w/w to plasma protein). SDC was removed after precipitation with 5 µl of 20% trifluoroacetic acid and centrifugation. Sixty µl was transferred to a PCR plate and frozen at -20°C until analysis.

Mouse HDL digestion. HDL (10 µg protein) was digested as previously described (Pamir et al., 2016). The HDL was diluted into 0.5% SDC (Sigma-Aldrich, USA) in 200 mM NH_4HCO_3, spiked with 0.05 µg of [^{15}N]APOA1 as internal standard, reduced with dithiothreitol, alkylated with iodoacetamide, and digested with two additions of trypsin (1:20, w/w HDL protein; sequencing grade, Promega, WI) for 4 h. After precipitation of SDC with formic acid (1% final concentration), samples were frozen and stored at −20°C until analysis (less than a week).

LC-MS/MS quantification of selected apolipoproteins in mouse plasma and in HDL. The abundance of selected proteins was quantified by mass spectrometry using data independent analysis (DIA), as previously described (Chait et al., 2020). After desalting on a C18 trapping column (Reprosil-Pur 120 C18-AQ, 5 µm, 0.1 x 40 mm, Dr. Maisch HPLC GmbH, Germany) at a flow rate of 4 µl/min, the digested peptides were separated on an analytical column (Reprosil-Pur 120 C18-AQ, 5 µm, 250x0.075 mm, Dr. Maisch HPLC GmbH). The following multi-step linear gradient was used: 1-5%B in 2 min, 5-25% in 50 min, 25-35% in 10 min. At the end, the gradient column was washed with a ramp to 80%B and re-equilibrated (A - 0.1% formic acid in water, B - acetonitrile, 0.1% formic acid, flow rate of 0.4 µl/min). An LC-MSMS consisting of a nanoAquity UPLC (Waters, MA), and a Thermo Fusion Lumos (Thermo Fisher, San Jose, CA) tribrid mass spectrometer with electrospray ionization was used for the analysis. DIA parameters were as follows: MS1 scan (395-1005 Da, resolution 120,000, maximum injection time 50 ms) followed with two sets of 30 MS/MS scans across 400-1000 Da range with 20 Da mass selection window each (resolution 15,000, maximum injection time 22 ms, loop time 3 sec) with 10 m/z overlap. Fragmentation was induced by HCD activation at a normalized collision energy of 30%. Further data processing was accomplished using Skyline (Maclean et al., 2010) to extract fragment ion chromatograms of the MS2 scans (the top 5 fragment ions for the peptides derived from proteins of interest) with 10 ppm accuracy windows. Chromatograms were integrated, and chromatographic peak areas were exported for further analysis. Relative quantification of individual proteins was accomplished using the ratio of the endogenous

peptide peak area to peak area of the corresponding SIL peptide. Abundance of other proteins was quantified after normalization of the representative peptides to the ^{15}N-APOA1 peptide VQPYLDDFQK. Peptide and protein abundance is therefore expressed in arbitrary units [a.u.]. The common denominator for plasma analysis was volume of plasma.

Digestion of human VLDL+IDL. Two micrograms of the VLDL+IDL proteins were diluted into 55 µl of 0.5% sodium deoxycholate, 5% acetonitrile in 100 mM ammonium bicarbonate. Samples were reduced and denatured by incubation with 5.5 mM DTT at 90°C for 60 min and alkylated with 19 mM iodoacetamide for 45 min in the dark. Addition of 5 µl of 100 mM DTT quenched unreacted iodoacetamide. The proteins were digested with trypsin (1:10, w/w, Promega, WI) for 18 h at 37°C. Digestion was stopped and SDC precipitated by addition of formic acid to pH <2.5 and a 30 min incubation. The SDC precipitate was removed by centrifugation and the supernatant was frozen until LC-MS/MS analysis.

LC-MS/MS analysis of human VLDL+IDL. Selected apolipoproteins (APOB100, APOB48, APOC2, APOC3, APOA4 and APOE) were quantified by targeted LC-MS/MS using selected reaction monitoring (SRM) on an EasyLC 1200 and TSQ Altis (Thermo Fisher, CA) LC-MS/MS instrument. After desalting on a C18 trapping column (Reprosil-Pur 120 C18-AQ, 5 µm, 0.1 x 40 mm, Dr. Maisch HPLC GmbH, Germany) at a flow rate of 4 µl/min, the digested peptides were separated on an analytical column (Reprosil-Pur 120 C18-AQ, 5 µm, 250x0.075 mm, Dr. Maisch HPLC GmbH). The following multi-step linear gradient was used: 1-9%B in 2 min, 9-31% in 17 min, 31-44% in 3 min. At the end of run, the gradient column was washed with a 2 min ramp to 100%B and re-equilibrated (A - 0.1% formic acid in water, B – 80% acetonitrile, 0.1% formic acid, flow rate of 0.4 µl/min). A scheduled SRM method was used to quantify peptides with at least 2 peptides per proteins and 3-5 transitions for each peptide (with the exception of APOB48 where a single specific peptide was quantified). The collision energy was specifically optimized for each peptide, and resolution was set to 2.0 FWHM for Q1 and 1.2 FWHM for Q3 and collision gas pressure of 1.5 mTorr. Data were further processed in Skyline, and the ratio of the endogenous peptide to SIL peptide was calculated as the response factor for each peptide.

Supplemental References

Chait A, den Hartigh L, Wang S, Goodspeed L, Babenko I, Altemeier WA, Vaisar T. Presence of serum amyloid A3 in mouse plasma is dependent on the nature and extent of the inflammatory stimulus. *Sci Rep*. 2020 Jun 25;10(1):10397.

Hutchins PM, Ronsein GE, Monette JS, Pamir N, Wimberger J, He Y, Anantharamaiah GM, Kim DS, Ranchalis JE, Jarvik GP, Vaisar T, Heinecke JW. Quantification of HDL particle concentration by calibrated ion mobility analysis. *Clin Chem.* 2014 Nov;60(11):1393-401.

Maclean B, Tomazela DM, Abbatiello SE, Zhang S, Whiteaker JR, Paulovich AG, Carr SA, Maccoss MJ. Effect of collision energy optimization on the measurement of peptides by selected reaction monitoring (SRM) mass spectrometry. *Anal Chem.* 2010 Dec 15;82(24):10116-24.

Pamir N, Hutchins P, Ronsein G, Vaisar T, Reardon CA, Getz GS, Lusis AJ, Heinecke JW. Proteomic analysis of HDL from inbred mouse strains implicates APOE associated with HDL in reduced cholesterol efflux capacity via the ABCA1 pathway. *J Lipid Res.* 2016 Feb;57(2):246-57.

Subramanian S, Han CY, Chiba T, McMillen TS, Wang SA, Haw A 3rd, Kirk EA, O'Brien KD, Chait A. Dietary cholesterol worsens adipose tissue macrophage accumulation and atherosclerosis in obese LDL receptor-deficient mice. *Arterioscler Thromb Vasc Biol*. 2008 Apr;28(4):685-91.

Supplemental Table 1. *CREB3L3* mutations

Age	Sex	Mutation	Ontology	Frequency	CADD
LOF					
56	M	CREB3L3:NM_032607:exon6:c.732dupG:p.L244fs	Frameshift	0.0003	-
66	M	CREB3L3:NM_032607:exon6:c.732dupG:p.L244fs	Frameshift	0.0003	
38	F	CREB3L3:NM_032607:exon6:c.732dupG:p.L244fs	Frameshift	0.0003	-
38	M	CREB3L3:NM_032607:exon10:c.G1208A:p.W403X	Nonsense (early truncation)	Not seen	-
24	M	CREB3L3:NM_032607:exon6:c.732dupG:p.L244fs	Frameshift	0.0003	-
Missense					
45	F	CREB3L3:NM_032607:exon6:c.G718A:p.E240K	Missense	Not seen	34
44	M	CREB3L3:NM_032607:exon6:c.C742T:p.R248C	Missense	0.0000323	34
45	M	CREB3L3:NM_032607:exon5:c.C704A:p.P235H	Missense	Not seen	26
72	M	CREB3L3:NM_032607:exon10:c.C1108A:p.R370S	Missense	Not seen	25.8
56	F	CREB3L3:NM_032607:exon4:c.G538A:p.V180M	Missense	6.47E-05	24.5

CADD score >20 indicates likely or probably deleterious; LOF, loss-of-function

Supplemental Table 2. Primer sequences

Gene	Gene name	Forward (5' - 3')	Reverse (5' - 3')
Rn18s	18s ribosomal RNA	CATTAAATCAGTTATGGTTCCTTTGG	CCCGTCGGCATGTATTAGCT
Abcg5	ATP binding cassette subfamily G member 5	ATCCAACACCTCTATGCTAAATCAC	TACATTATTGGACCAGTTCAGTCAC
Abcg8	ATP binding cassette subfamily G member 8	CCTCATCATTGGCTTCCTTAC	ATTGACCTCTCCGAGTGACATT
Angptl3	angiopoietin like 3	ACATGTGGCTGAGATTGCTG	GCTGGAGCATCATTTTGGAT
Angptl4	angiopoietin like 4	GGAAAAGATGCACCCTTCAA	TGCTGGATCTTGCTGTTTTG
Angptl8	angiopoietin like 8	GTGCTGCAAGGAACACTGAA	TCCACAGGGCTCTGTCTTCT
Apoa1	apolipoprotein A-I	CAT GCG CAC ACA CGT AGA CT	CTC GCC AAG TGT CTT CAG GT
Apoa4	apolipoprotein A-IV	AAAGTAACCCAGACGTTCGGG	CGCTGGATGTATGGGGTCAG
Apoa5	apolipoprotein A-V	AGGCAGCAGTTGAAACCCTA	TGAGCCTTGGTGTCTTCCTCC
Apob	apolipoprotein B100	CACCACATGGGAGCACAATA	CCACCTTTCCAGCTGATC TT
Apoc2	apolipoprotein C-II	GAGCCAGGATAGTCCCTTCC	AAAATGCCTGCGTAAGTGCT
Apoc3	apolipoprotein C-III	TACAGGGCTACATGGAACAAGC	CAGGGATCTGAAGTGATTGTCC
Apoe	apolipoprotein E	TCTGACCAGGTCCAGGAAGAG	CATCAGTGCCGTCAGTTCTTG
Cidec	cell death inducing DFFA like effector C	ATGGACTACGCCATGAAGTCT	CGGTGCTAACACGACAGGG
Cpt1a	carnitine palmitoyltransferase 1a	ACCACTGGCCGCATGTCAAG	CAGCGAGTAGCGCATAGTCA
Creb3l3	cAMP-responsive element binding protein3 like 3	CCAGAGCCCTTTACCCATACAT	ATGGTTGGAGGTTAGGGTTCAG
Creb3l3 (AAV-derived)		TAGCGGGCCCTCTAGAC	GGCGCCATAGCACAGAC
Fasn	fatty acid synthase	TTCCAAGACGAAAATGATGC	AATTGTGGGATCAGGAGAGC
Fgf21	fibroblast growth factor 21	CCCTGATGGAATGGATGAGA	TGGGCTTCAGTGTCTTGGTC
Lipc	hepatic lipase	GACGGG AAGAACAAGATTGGAA	TTGGCATCAGGAGAAAGG
Lpl	lipoprotein lipase	GTGGCCGAGAGCGAGAACAT	GC TTTCACTCGGATCCTCTC
Lrp1	LDL receptor-related protein 1	TGGTCTGATGTGCGGACTCA	AACAGATTTCGGGAGACCCA
Lxra	liver X receptor alpha	ATCGCCTTGCTGAAGACCTCTG	GATGGGGTTGATGAACTCCACC
Mttp	microsomal triglyceride transfer protein	AGCTTTGTCACCGCTGTGC	TCCTGCTATGGTTTGTTGGAAGT
Ppara	peroxisome proliferator-activated receptor alpha	GGCCTGGCCTTCTAAACATA	GTCGGACTCGGTCTTCTTGA
Sdc1	syndecan1	AGGATGGAACTGCCAATCAG	ATCCGGTACAGCATGAAAGC
Vldlr	VLDL receptor	TTCCTAGCTCATCCTCTTGCAC	CTGACCCAGTGAATTTATTGGC

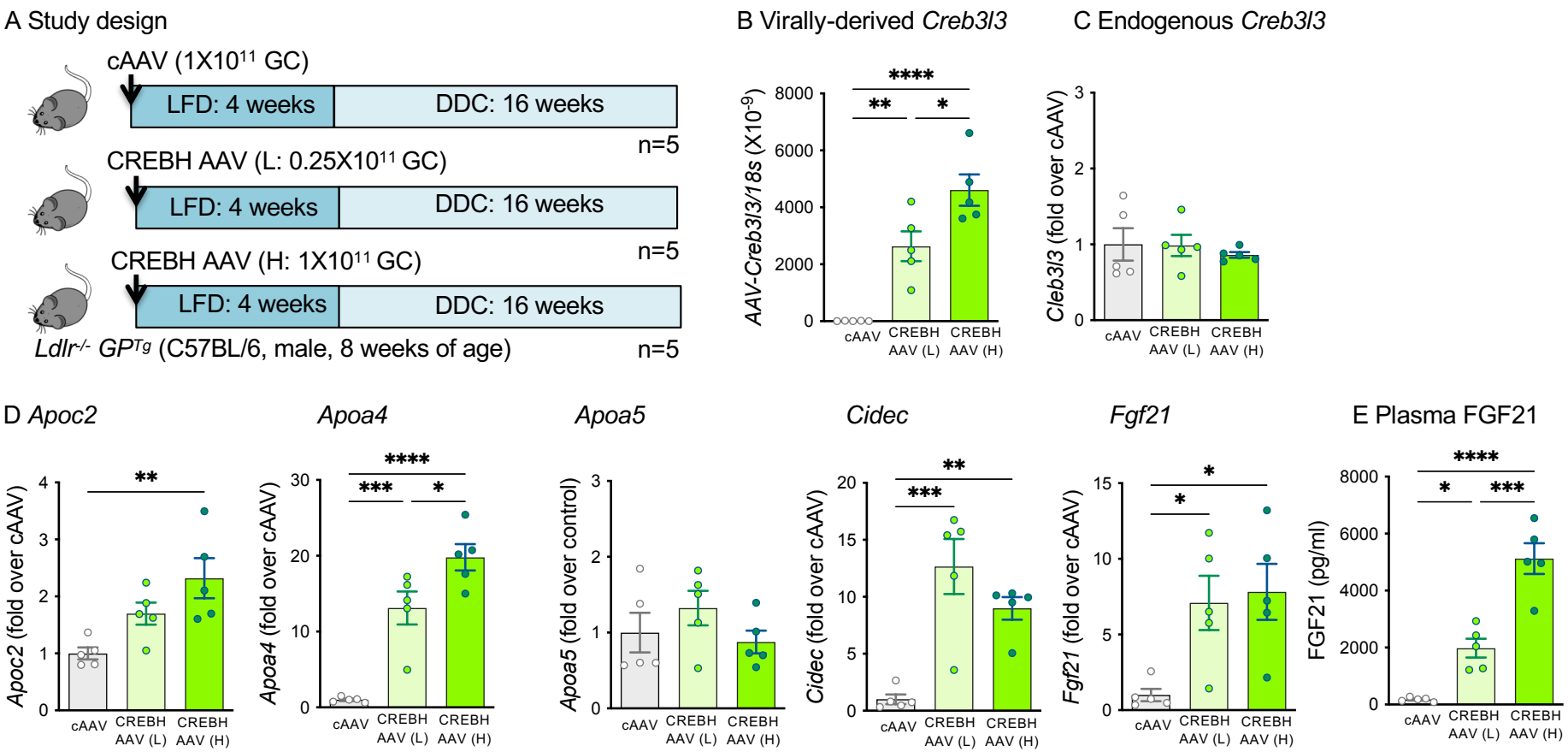

Supplemental figure 1. Liver-specific expression of active CREBH dose-dependently elevates hepatic target gene expression. (A) Male *Ldlr*$^{-/-}$*;Gp*^{Tg} mice were fed a low-fat, semi-purified diet (LFD) and after one week were injected with cAAV (control empty AAV DJ/8, 1X10^{11} GC), a low dose of CREBH AAV (L: 0.25X10^{11} GC) or a high dose of CREBH AAV (H: 1X10^{11} GC). The mice were maintained on the low-fat semi-purified diet for an additional 4 weeks and were then switched to a diabetogenic diet with added cholesterol (DDC) and maintained for another 16 weeks. At the end of the study, livers were collected and used for measurement of mRNA levels. (B-C) AAV-derived *Creb3l3* mRNA is expressed as relative expression to *Rn18s* and endogenous *Creb3l3* mRNA is expressed as ddCT (fold over cAAV). (D) *Apoc2*, *Apoa4*, *Apoa5*, *Cidec*, and *Fgf21* mRNA levels are expressed as ddCT (fold over cAAV). (E) Plasma was used for measurements of FGF21 by ELISA. Mean ± SEM (n=5), *p<0.05, **p<0.01, ***p<0.001, ****p<0.0001, one-way ANOVA followed by Tukey's multiple comparisons tests.

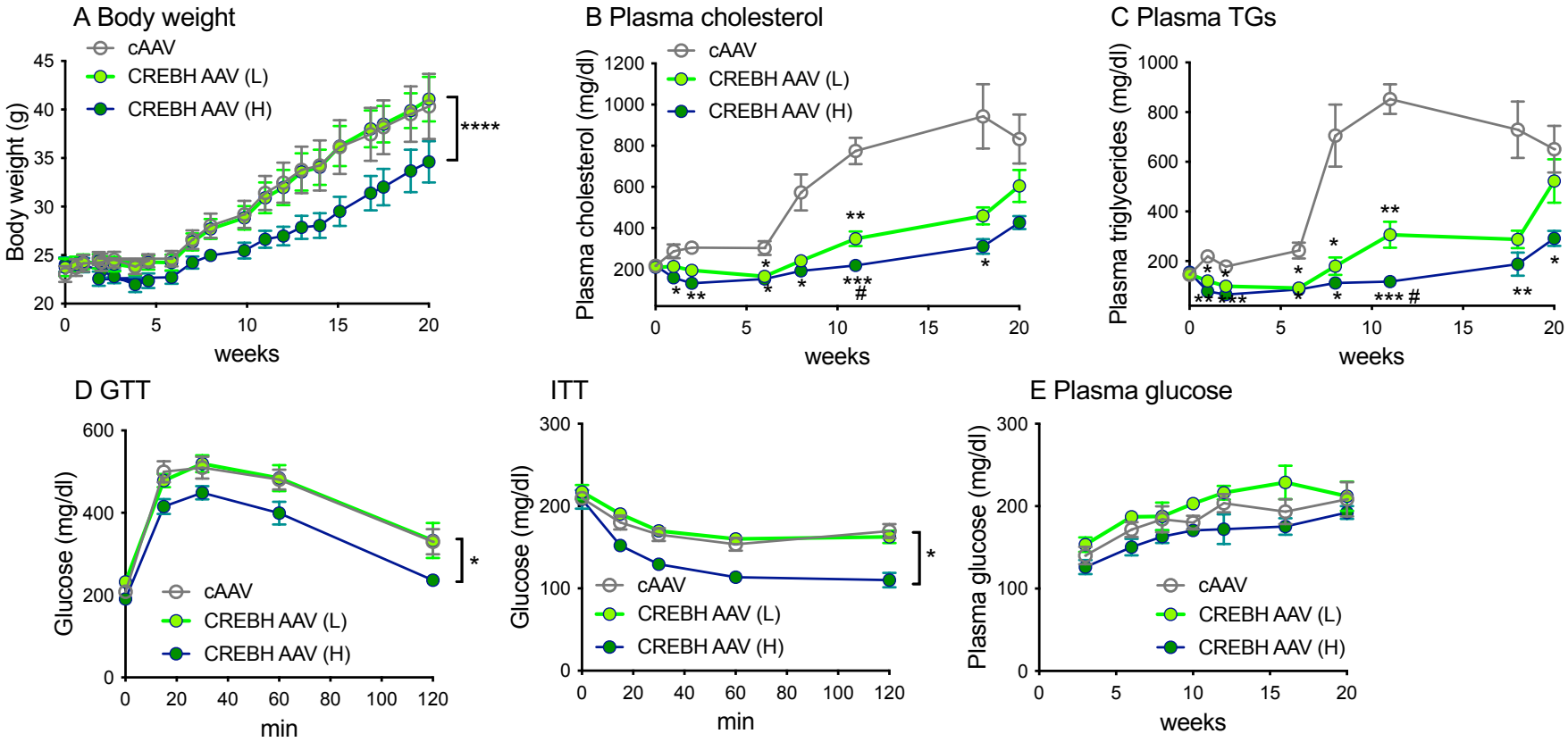

Supplemental figure 2. Liver-specific expression of active CREBH dose-dependently prevents body weight gain and improves hyperlipidemia and glucose- and insulin-tolerance in a mouse model of pre-diabetes. Male *Ldlr*$^{-/-}$*;Gp*^{Tg} mice were fed a low-fat, semi-purified diet (LFD) and after one week were injected with cAAV (control empty AAV DJ/8, 1X10^{11} GC), a low dose of CREBH AAV (L: 0.25X10^{11} GC) or a high dose of CREBH AAV (H: 1X10^{11} GC). The mice were maintained on the low-fat semi-purified diet for an additional 4 weeks and were then switched to a diabetogenic diet with added cholesterol (DDC) and maintained for another 16 weeks. (A) Body weight was monitored at the indicated times. Plasma cholesterol (B) and TG (C) were monitored at indicated time-points. (D) Glucose tolerance tests (GTT) were performed at week 12 of DDC and insulin tolerance tests (ITT) were performed two weeks later, at week 14 of DDC. (E) Non-fasting plasma glucose levels throughout the study. Mean ± SEM (n=5), *p<0.05, **p<0.01, ***p<0.001, ****p<0.0001 (vs cAAV), $^{\#}$p<0.01 (vs CREBH AAV L), one-way ANOVA followed by Tukey's multiple comparisons tests.

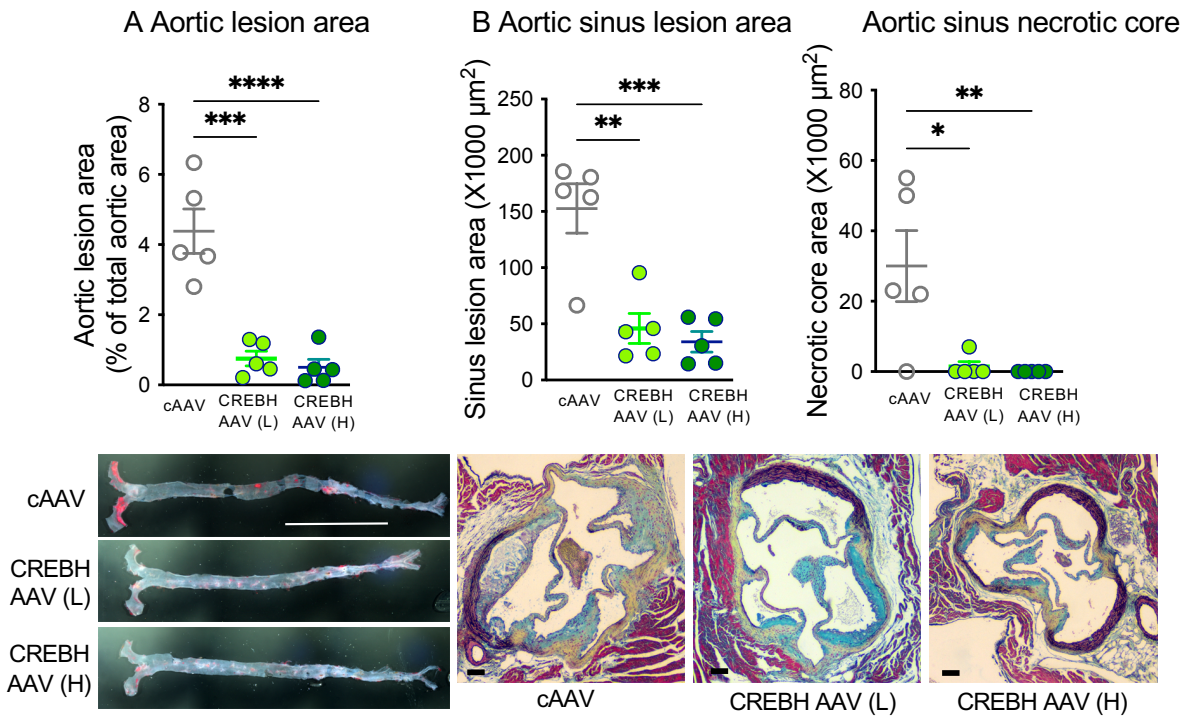

Supplemental figure 3. Liver-specific expression of active CREBH prevents the formation of atherosclerotic lesions in a mouse model of pre-diabetes. Male *Ldlr*$^{-/-}$*;Gp*^{Tg} mice were fed a low-fat, semi-purified diet (LFD) and after one week were injected with cAAV (control empty AAV DJ/8, 1X10^{11} GC), a low dose of CREBH AAV (L: 0.25X10^{11} GC) or a high dose of CREBH AAV (H: 1X10^{11} GC). The mice were maintained on the low-fat semi-purified diet for an additional 4 weeks and were then switched to a diabetogenic diet with added cholesterol (DDC) and maintained for another 16 weeks. At the end of the study, aortas and hearts were collected for analysis of atherosclerotic lesions. The aorta was longitudinally opened and stained with Sudan IV. The red lipid-rich plaque area was quantified (A, bottom: representative images, scale bar is 1 cm). Aortic sinus sections were stained with a Movat's pentachrome stain and used to quantify the size of total lesion and necrotic core (B, bottom: representative images, scale bar is 100 µm). Mean ± SEM (n=5), *p<0.05, **p<0.01, ***p<0.001, ****p<0.0001, one-way ANOVA followed by Tukey's multiple comparisons tests.

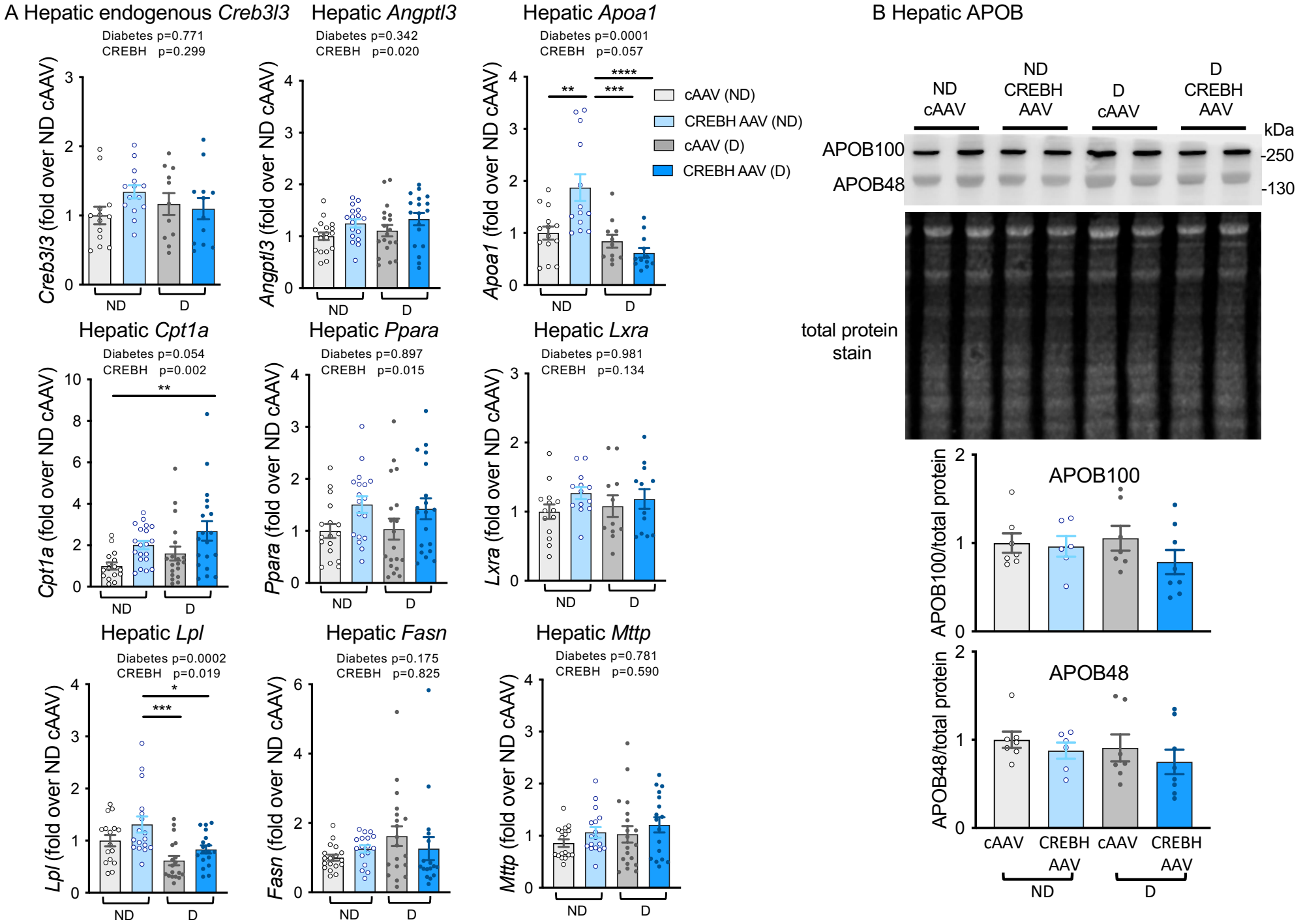

Supplemental figure 4. Characterization of hepatic expression of genes involved in lipid metabolism and APOB protein levels in mice expressing active CREBH.

C Intestinal AAV-derived *Creb3l3* Intestinal *Creb3l3* Intestinal *Apoa4*

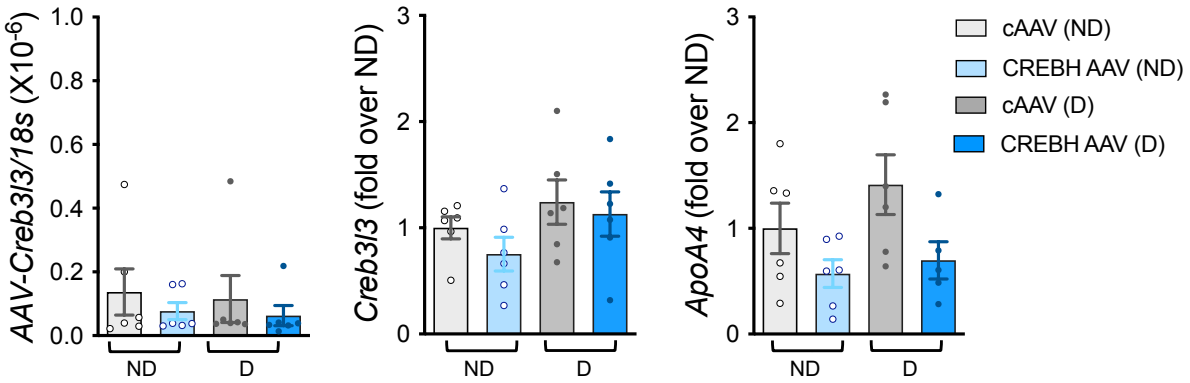

Continued, Supplemental figure 4. Characterization of hepatic expression of genes involved in lipid metabolism and APOB protein levels in mice expressing active CREBH. Male *Ldlr*$^{-/-}$*;Gp*^{Tg} mice were fed a high-fat diet for 16 weeks followed by chow for one week. Empty control AAV-DJ/8 (cAAV, 5X10^{10} GC) or AAV-DJ/8 containing the active form of mouse CREBH (CREBH AAV, 5X10^{10} GC) was then injected. One week later, the mice were injected with lymphocytic choriomeningitis virus (LCMV) to induce diabetes or with saline for non-diabetic controls. At the time of LCMV injection, the mice were switched to a low-fat, semi-purified diet and maintained for 4 weeks after the onset of diabetes. At the end of the study, liver samples (A) were collected for measurements of mRNAs of *Creb3l3* (endogenous), *Angptl3*, *Apoa1*, *Ppara*, *Cpt1a, Lxra, Lpl, Mttp* and *Fasn* (n=17 ND cAAV, n=16 ND CREBH AAV, n=18 D cAAV, n=17 D CREBH AAV). Liver samples were also used for determination of APOB100 and APOB48 protein levels by immunoblot (B). Whole liver lysates (12 µg protein/lane) were separated on SDS-gels and transferred onto nitrocellulose membranes. The membranes were stained with total protein stain-700 (LI-COR) for normalization, then blocked in 5% milk in TTBS and blotted with rabbit anti-APOB (Abcam, ab20737). After incubation with anti-rabbit secondary antibody conjugated with HRP and ECL substrate (SuperSignal West Femto, Thermofisher) were used for detection of proteins. The signal intensities of APOB100 and APOB48 were quantified using LI-COR Image Studio software (n=7 ND cAAV, n=6 ND CREBH AAV, n=7 D cAAV, n=8 D CREBH AAV). *S*mall intestine (C) was collected for measurements of AAV-derived *Creb3l3*, endogenous *Creb3l3*, and *Apoa4 (*n=6). ND, non-diabetic mice; D, diabetic mice. Mean ± SEM, *p<0.05, **p<0.01, ***p<0.001, ****p<0.0001, two-way ANOVA followed by Tukey's multiple comparisons tests.

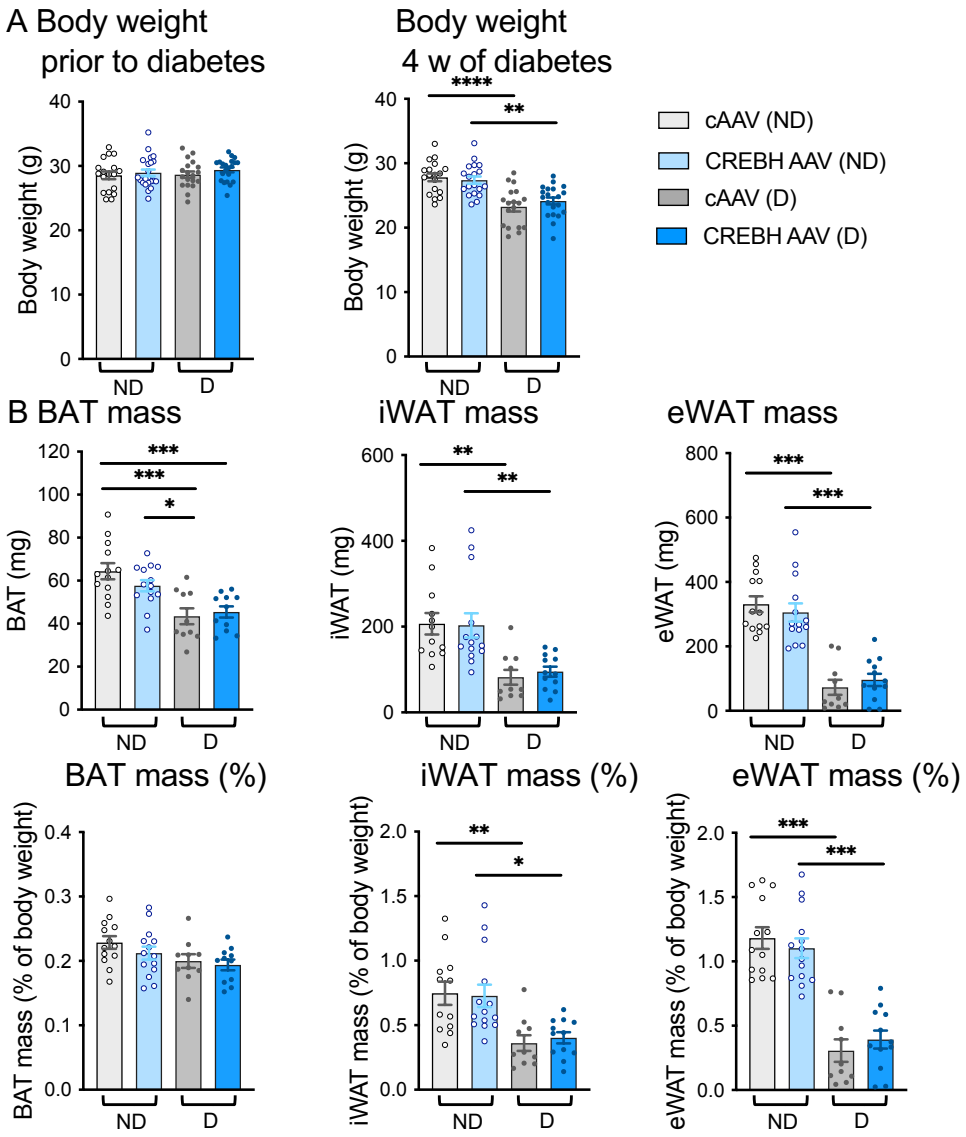

Supplemental figure 5. Hepatic CREBH expression does not affect body weight or adiposity. Male *Ldlr*$^{-/-}$*;Gp*^{Tg} mice were fed a high-fat diet for 16 weeks followed by chow for one week. Empty control AAV-DJ/8 (cAAV, 5X10^{10} GC) or AAV-DJ/8 containing the active form of mouse CREBH (CREBH AAV, 5X10^{10} GC) was then injected. One week later, the mice were injected with lymphocytic choriomeningitis virus (LCMV) to induce diabetes or with saline for non-diabetic controls. At the time of LCMV injection, the mice were switched to a low-fat, semi-purified diet and maintained for 4 weeks after the onset of diabetes. (A) Body weight was measured at the time of LCMV injection (prior to diabetes development) and one day before euthanasia (4 weeks of diabetes) (n=17 ND cAAV, n=16 ND CREBH AAV, n=18 D cAAV, n=17 D CREBH AAV). (B) At the end of the study, unilateral brown adipose tissue (BAT), inguinal white adipose tissue (iWAT) and epididymal white adipose tissue (eWAT) were collected and wet tissue weight was measured. Mass and percent body weight are shown (n=13 ND cAAV, n=14 ND CREBH AAV, n=10 D cAAV, n=12 D CREBH AAV). ND, non-diabetic mice; D, diabetic mice. Mean ± SEM, *p<0.05, **p<0.01, ***p<0.001, ****p<0.0001, two-way ANOVA followed by Tukey's multiple comparisons tests.

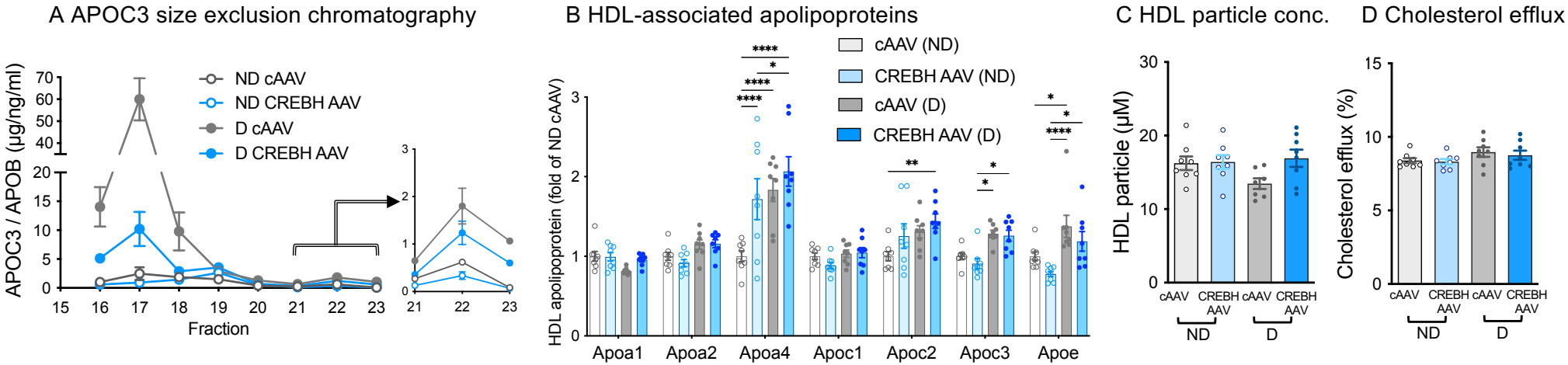

Supplemental figure 6. Effect of hepatic CREBH on lipoproteins. Male *Ldlr*$^{-/-}$*;Gp*^{Tg} mice were fed a high-fat diet for 16 weeks followed by chow for one week. Empty control AAV-DJ/8 (cAAV, 5X10^{10} GC) or AAV-DJ/8 containing the active form of mouse CREBH (CREBH AAV, 5X10^{10} GC) was then injected. One week later, the mice were injected with lymphocytic choriomeningitis virus (LCMV) to induce diabetes or with saline for non-diabetic controls. At the time of LCMV injection, the mice were switched to a low-fat, semi-purified diet and maintained for 4 weeks after the onset of diabetes. (A) At the end of the study, plasma samples were separated by FPLC (pooled plasma of 2-3 mice/n, n=3/group). APOB and APOC3 were measured by ELISA in fractions (#16-23; fractions containing VLDL, IDL and LDL). The relative levels of APOC3 in fractions were normalized to APOB, providing an estimate of APOC3 molecules/lipoprotein particle. Mean ± SD. (B) HDL was isolated by sequential density ultracentrifugation (d= 1.063–1.21 mg/ml), tryptically digested and analyzed by targeted mass spectrometry. (C) HDL particle concentration was measured by calibrated ion mobility analysis. (D) HDL's cholesterol efflux capacity was measured in J774 cells stimulated with cAMP to induce expression of cholesterol transporters, using the same concentration of HDL particles/assay (~4 µg). ND, non-diabetic mice; D, diabetic mice. Mean ± SEM (n=8) *p<0.05, **p<0.01, ***p<0.001, ****p<0.0001, two-way ANOVA followed by Tukey's multiple comparisons tests.

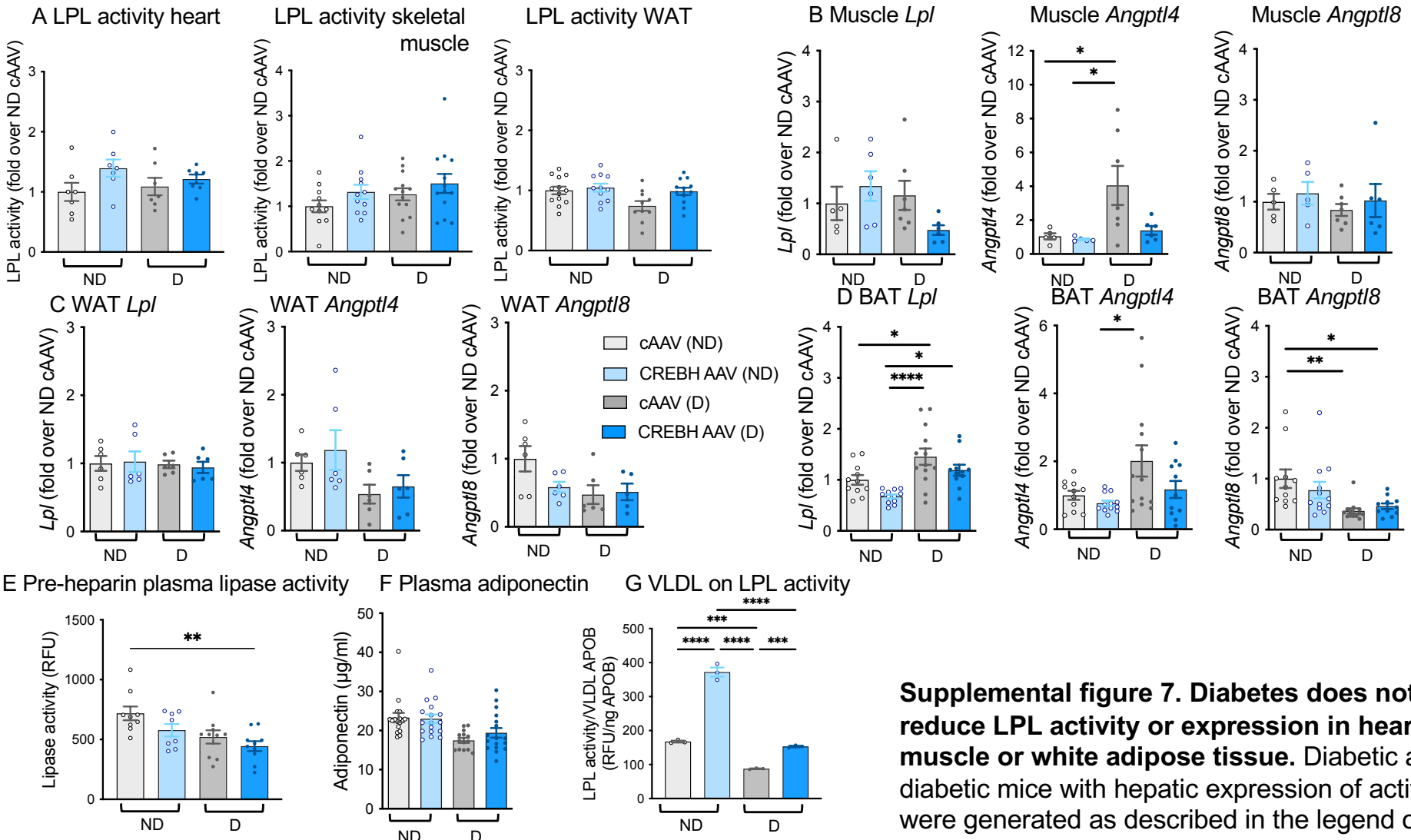

Supplemental figure 7. Diabetes does not directly reduce LPL activity or expression in heart, skeletal muscle or white adipose tissue. Diabetic and non-diabetic mice with hepatic expression of active CREBH were generated as described in the legend of figure 1. (A) At the end of the study, heart, skeletal muscle (hindlimb muscle), and white adipose tissue (inguinal WAT) were collected for measurements of heparin-releasable tissue LPL activity (heart: n=7 ND cAAV, n=7 ND CREBH AAV, n=7 D cAAV, n=7 D CREBH AAV; skeletal muscle, n=11, n=11, n=13, n=13; WAT, n=13, n=11, n=10, n=12). (B-D) Skeletal muscle, WAT and brown adipose tissue (BAT) mRNAs of *Lpl*, *Angptl4* and *Angptl8* (skeletal muscle, n=5 ND cAAV, n=6 ND CREBH AAV, n=7 D cAAV, n=6 D CREBH AAV; WAT, n=6, n=6, n=6, n=6; BAT, n=11, n=12, n=13 n=11). (E) Pre-heparin plasma lipase activity (largely hepatic lipase). Diabetes had a significant overall inhibitory effect (p=0.003) and CREBH also modestly reduced lipase activity (p=0.046) by two-way ANOVA (n=9 ND cAAV, n=8 ND CREBH AAV, n=10 D cAAV, n=10 D CREBH AAV). (F) Plasma adiponectin was measured by ELISA (n=17 ND cAAV, n=16 ND CREBH AAV, n=14 D cAAV, n=17 D CREBH AAV), Mean ± SEM . (G) Human recombinant LPL was incubated with VLDL isolated by size-exclusion chromatography. The activity was measured with EnzChek fluorescent LPL substrates and normalized to APOB content in the VLDL (n=3), Mean ± SD. ND, non-diabetic mice; D, diabetic mice. *p<0.05, **p<0.01, ***p<0.001, ****p<0.0001, two-way ANOVA followed by Tukey's multiple comparisons tests.

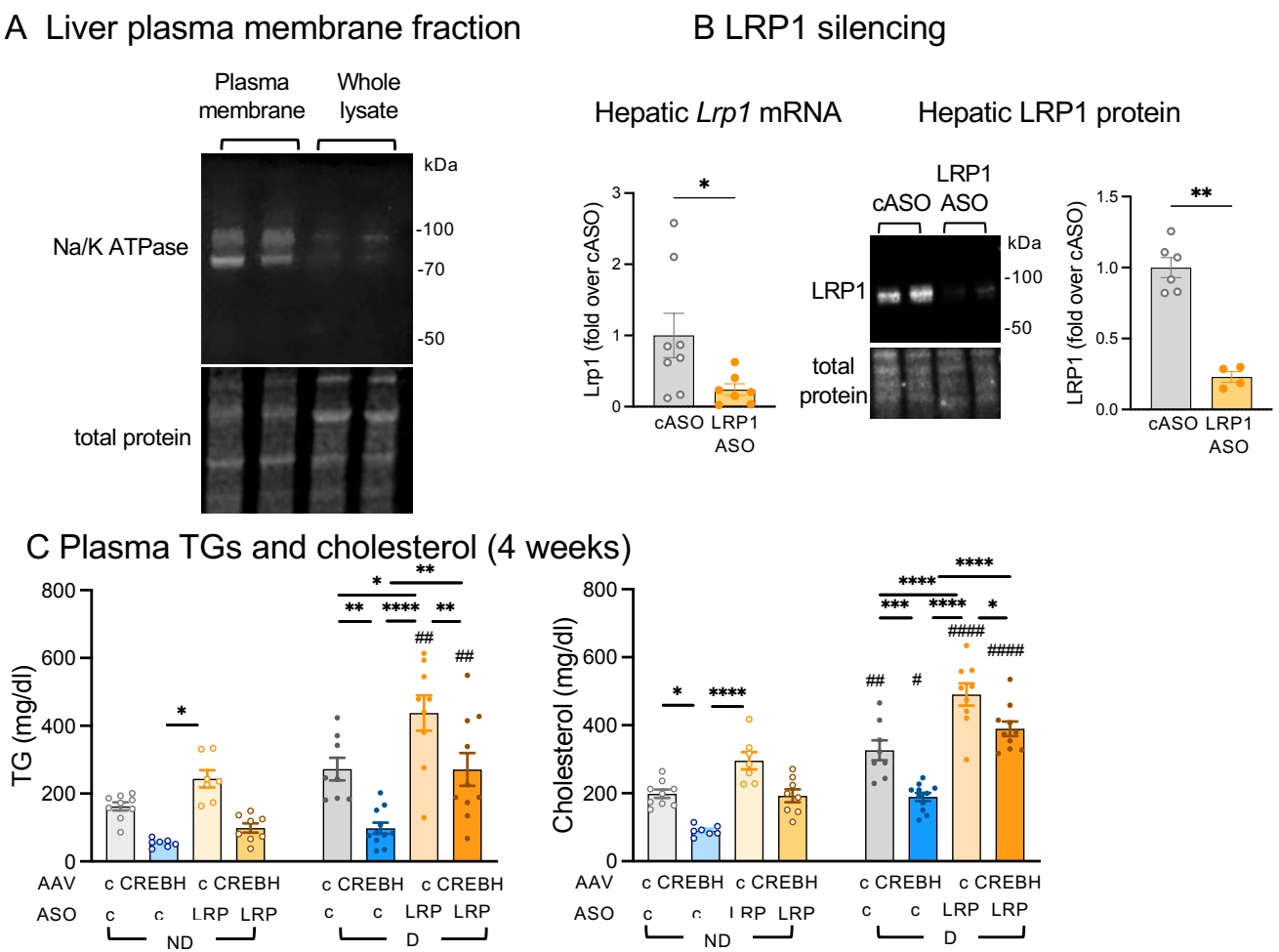

Supplemental figure 8. Liver-targeted silencing of LRP1 by a GalNAc LRP1 ASO. (A) A plasma membrane enrichment kit (Invent Biotechnologies) was used to enrich plasma membranes from whole liver lysates. The enrichment of plasma membranes following isolation by the kit, as compared with whole liver lysates, was verified by immunoblot of Na/K ATPase as a plasma membrane marker protein. (B) The effectiveness of LRP1 ASO to silence LRP1 was verified in livers of non-diabetic mice injected with the liver-targeted LRP1 GalNAc ASO and maintained for 4 weeks. Hepatic *Lrp1* mRNA was measured by real-time PCR (n=8 cASO, n=7 LRP1 ASO). Liver whole lysates were used for immunoblot analysis of LRP1 (n=6 cASO, n=4 LRP1 ASO). Mean ± SEM *p<0.05, **p<0.01, Mann-Whitney tests. (C) *Ldlr*$^{-/-}$ mice were were injected with CREBH AAV or cAAV (5X10^{10} GC) and LCMV injected a week later. Mice were treated with LRP1 ASO or cASO once a week for 4 weeks from the onset of diabetes. Plasma TG and cholesterol were measured at week 4 after induction of diabetes. ND, non-diabetic mice; D, diabetic mice. Mean ± SEM *p<0.05, **p<0.01, ***p<0.001, ****p<0.0001, two-way ANOVA followed by Tukey's multiple comparisons tests. #p<0.05, ##p<0.01, ###p<0.001, ####p<0.0001 denote significance versus the corresponding non-diabetic group (n=9 ND cAAV cASO, n=7 ND CREBH AAV cASO, n=7 ND cAAV LRP1 ASO, n=8 ND CREBH AAV LRP1 ASO, n=8 D cAAV cASO, n=11 D CREBH AAV cASO, n=9 D cAAV LRP1 ASO, n=10 D CREBH AAV LRP1 ASO).

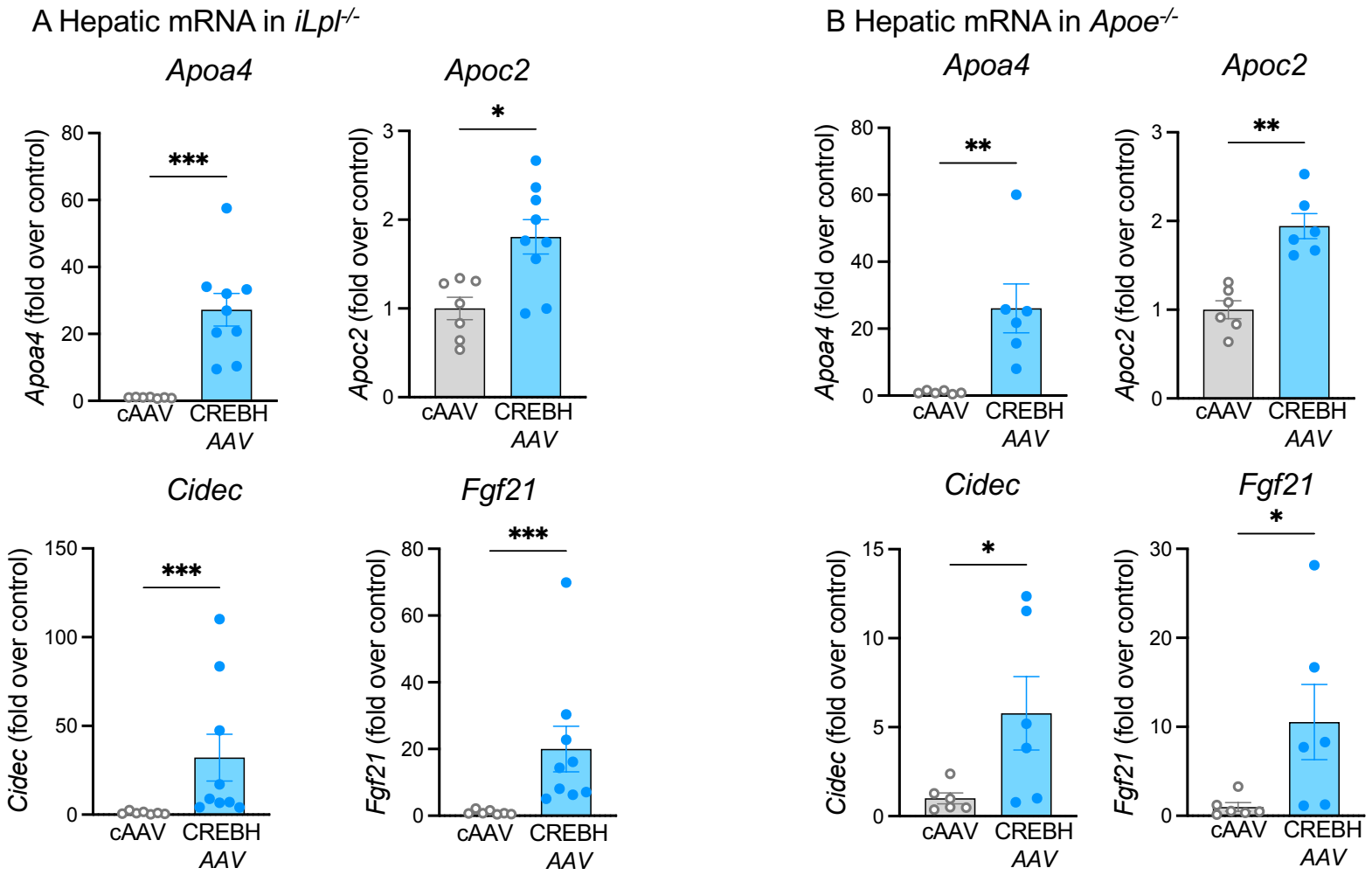

Supplemental figure 9. Active CREBH expression induces its target genes in *iLpl*$^{-/-}$ mice and *Apoe*$^{-/-}$ mice. (A) *iLpl*$^{-/-}$ mice were injected with empty control AAV8 (cAAV, 2X10^{11} GC) or AAV8 containing the active form of mouse CREBH (CREBH AAV, 2X10^{11} GC). Four weeks later, the livers were collected for determination of mRNA (n=7 cAAV, n=9 CREBH AAV). (B) Male *Apoe*$^{-/-}$ mice were fed a low-fat diet for 1 week before empty control AAV8 (cAAV, 2X10^{11} GC) or AAV8 containing the active form of mouse CREBH (CREBH AAV, 2X10^{11} GC) was injected. The mice then fed the low-fat diet for 3 weeks. At the end of the study, the livers were collected for determination of mRNA (n=6). Mean ± SEM *p<0.05, **p<0.01, ***p<0.001, Mann-Whitney tests.

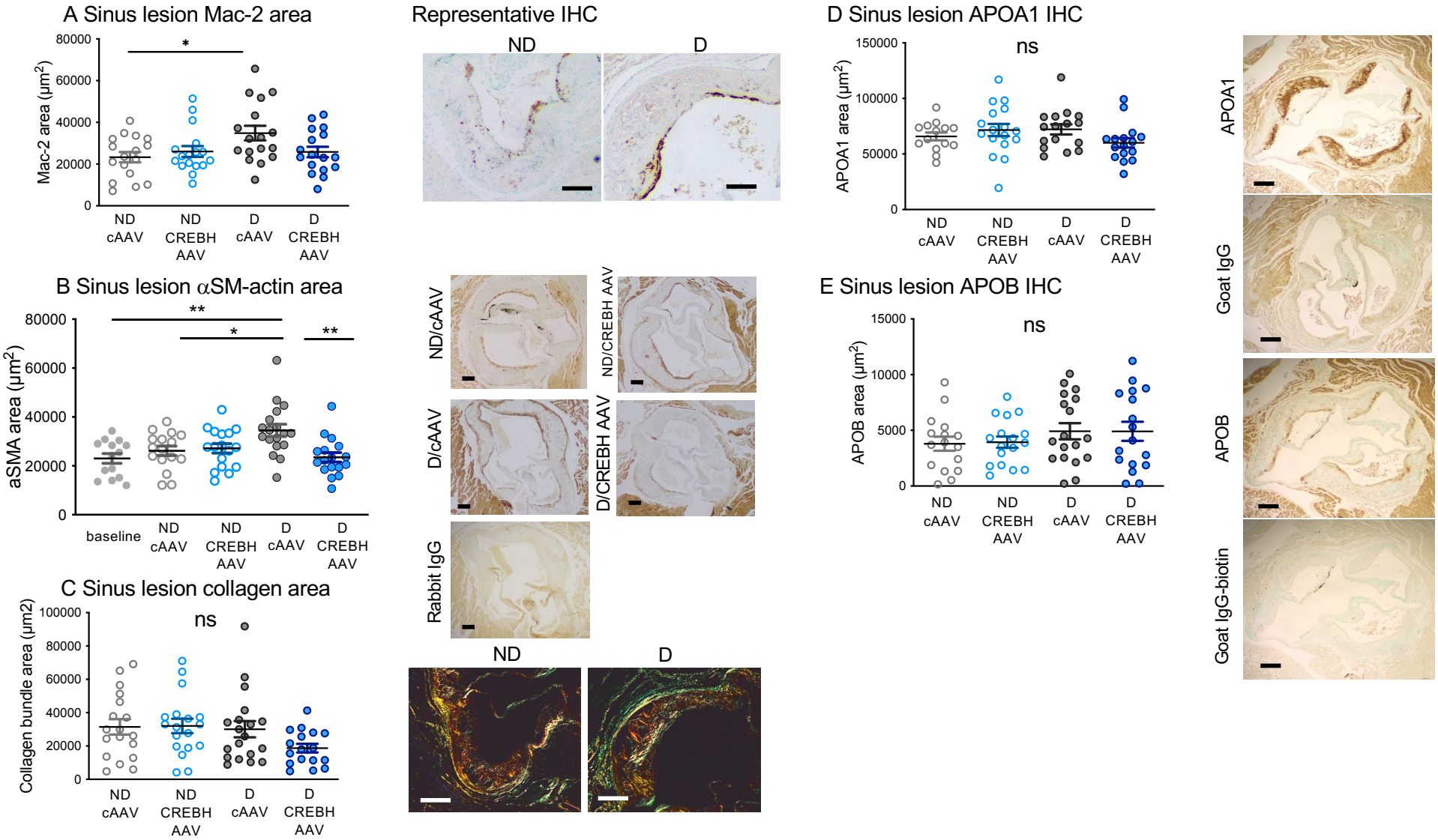

Supplemental figure 10. Diabetes increases macrophage and α-smooth muscle actin-positive cells in sinus lesions. Diabetic and non-diabetic mice expressing CREBH (CREBH AAV) or injected with a control (cAAV) were generated as described in the legend of figure 1. After 4 weeks of diabetes, mice were euthanized, and aortic sinus lesions were immunostained for Mac-2 as a marker of macrophages (A), α-smooth muscle actin as a marker of a smooth muscle cell population (B), picosirius red to evaluate collagen (C), APOA1 (D) and APOB (E). Goat IgG and Goat IgG conjugated with biotin were used for negative controls for APOA1 and APOB immunostaining, respectively. Representative images are shown. The amount of positive staining was quantified. ND, non-diabetic mice; D, diabetic mice. Mean ± SEM (n=17 ND cAAV, n=16 ND CREBH AAV, n=18 D cAAV, n=17 D CREBH AAV), ns; not significant, one-way ANOVA followed by Tukey's multiple comparisons tests. Scale bar is 100 μm.

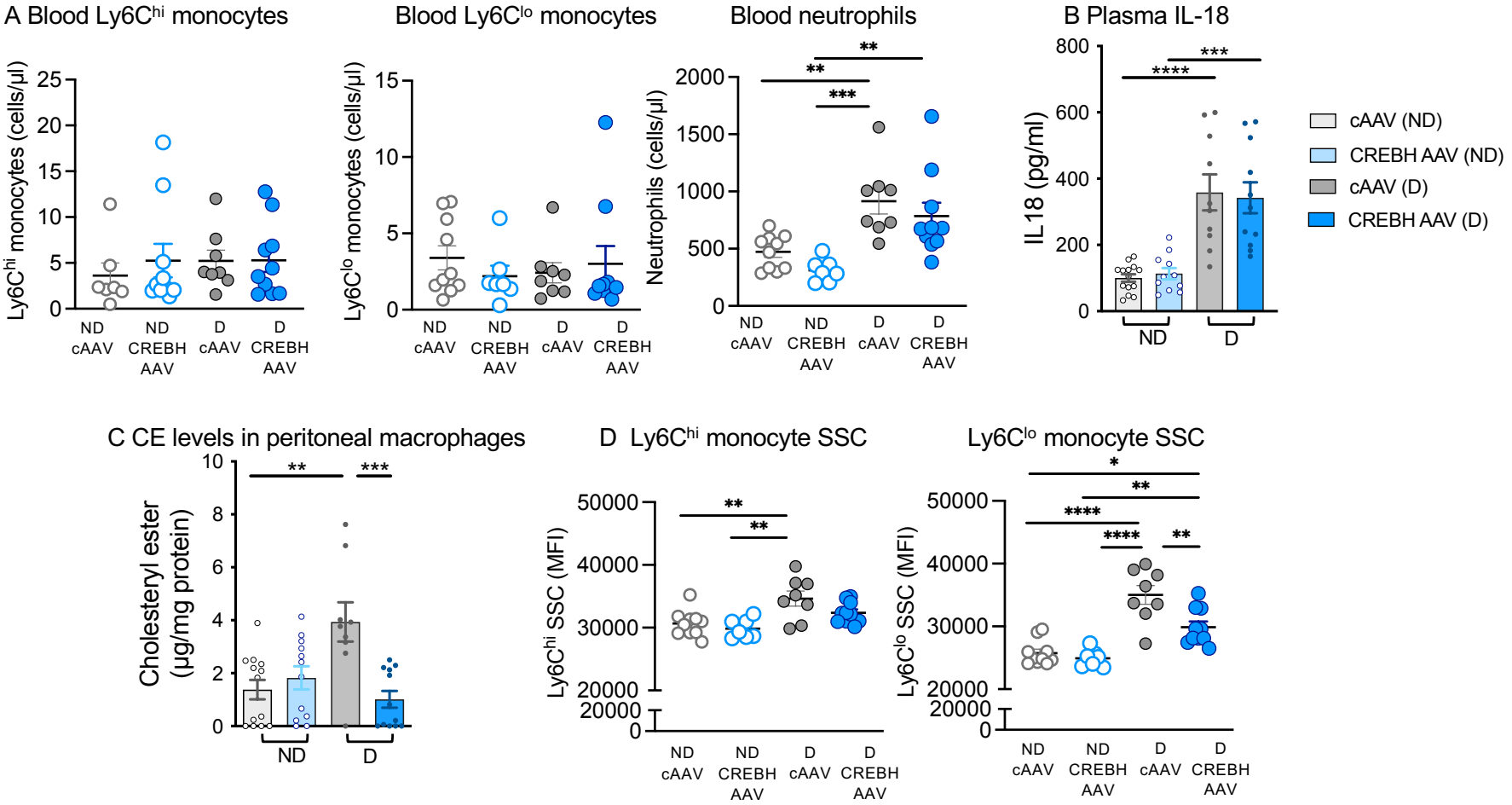

Supplemental figure 11. Diabetes causes increased lipid loading of macrophages and Ly6C^{lo} monocytes through a process prevented by hepatic CREBH expression. Diabetic and non-diabetic mice with CREBH overexpression (CREBH AAV) and mice injected with control empty AAV (cAAV) were maintained for 4 weeks. (A) Circulating monocytes (Ly6C^{hi} and Ly6C^{lo} populations) and neutrophils were measured by flow cytometry using anti-CD45 (pan-leukocyte marker), anti-CD115 (monocyte marker) and anti-GR1 (Ly6C marker) (n=10 ND cAAV, n=7 ND CREBH AAV, n=8 D cAAV, n=10 D CREBH AAV). (B) Plasma IL-18 levels were measured at the end of the study by ELISA. (C) Peritoneal macrophages were collected at the end of the study. The contents of cholesteryl ester (CE) were measured using an Amplex Red kit (n=13 ND cAAV, n=12 ND CREBH AAV, n=9 D cAAV, n=12 D CREBH AAV). (D) Side-scatter of blood Ly6C^{hi} and Ly6C^{lo} monocytes as a marker of lipid loading (n=10 ND cAAV, n=7 ND CREBH AAV, n=8 D cAAV, n=10 D CREBH AAV). ND, non-diabetic mice; D, diabetic mice. Mean ± SEM , *p<0.05, **p<0.01, ***p<0.001, ****p<0.0001, two-way ANOVA followed by Tukey's multiple comparisons tests.